ChemComm

Cite this: *Chem. Commun.*, 2011, **47**, 10407–10409

www.rsc.org/chemcomm

COMMUNICATION

A near-infrared fluorescent calcium probe: a new tool for intracellular multicolour Ca^{2+} imaging†

Akihiro Matsui,[a] Keitaro Umezawa,[b] Yutaka Shindo,[b] Tomohiko Fujii,[b] Daniel Citterio,[a] Kotaro Oka*[b] and Koji Suzuki*[a]

Received 6th July 2011, Accepted 27th July 2011
DOI: 10.1039/c1cc14045k

We report a novel near-infrared fluorescent calcium probe (KFCA), which has good optical properties such as intense NIR fluorescence emission (670 nm, QY: 0.24), excellent ON/OFF ratio (120-fold), and good wavelength-compatibility with visible-light-emissive fluorophores (Fluo-4, DsRed2), and which is applicable for real-time dual-colour intracellular Ca^{2+} imaging.

Since the first establishment of fluorescent indicators for calcium ions (Ca^{2+}) in the 1980's[1] that had a great impact on physiological Ca^{2+} imaging, several new types of revolutionary fluorescent calcium probes (*e.g.* genetically encoded Ca^{2+} sensors,[2] two-photon Ca^{2+} probes[3]) have been developed in order to satisfy the increasing demands and interest in calcium imaging, as well as for the development of fluorescence imaging technology. However, one type of fluorescent probe, which is required for one of the cutting-edge topics in bioimaging, has not been well established, yet. That is, a near-infrared (NIR: 650–900 nm) fluorescent calcium probe. NIR probes are expected to enable significant improvements in simultaneous imaging of multiple targets in combination with typical visible-light-emitting fluorophores for interaction studies, which is one of the hottest recent research fields.[4–6] Furthermore, they are also applicable to *in vivo* fluorescence imaging of tissues, organs, and living animals.[7] Despite this high potential, there are presently only few NIR calcium probes reported based on cyanine[8] or squaraine[9] chromophores, with limited optical characteristics such as low quantum yield (ϕ) or poor ON/OFF fluorescence signal contrast. To the best of our knowledge, no application data for physiological Ca^{2+} imaging using these probes have been reported to date.

In this study, a novel NIR fluorescent Ca^{2+} probe (KFCA, see Fig. 1a and Scheme S1 in the ESI†) is described. This probe is composed of two moieties, a fluorescent moiety and a Ca^{2+} binding moiety. As the fluorescent moiety, one of the new

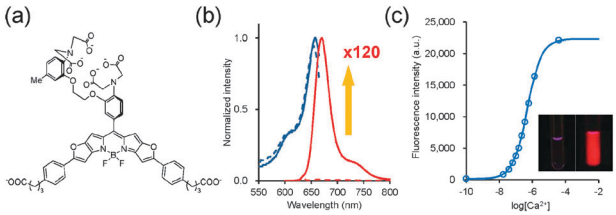

Fig. 1 (a) Chemical structure of KFCA. (b) Normalized absorption (blue) and fluorescence emission (red) spectra of KFCA in the absence (0 μM, dotted line) and presence (39 μM, solid line) of Ca^{2+}; excitation: 635 nm. (c) Ca^{2+}-concentration-dependent response curve of KFCA in buffer solution (see the ESI†). Circle plots represent the fluorescence intensity of KFCA at varying Ca^{2+} concentrations (0–39 μM). The solid line is based on a curve fitting with a theoretically calculated equilibrium constant assuming a 1 : 1 complex formation. The inset pictures show the emission of KFCA in the absence (0 μM, left) and presence (39 μM, right) of Ca^{2+} observed under 365 nm UV irradiation.

BODIPY-based KFL-fluorophores previously developed in our laboratory was chosen, due to the good optical properties such as sharp fluorescence spectra with high extinction coefficients and high quantum yields, as well as the fine-tuning ability of the absorption/emission spectral bands in the visible-NIR region.[10,11] On the basis of these findings, KFL-5 was selected from the KFL library.[11] Its absorption/emission spectral peaks (650/660 nm) are almost identical to those of Cy5 (649/670 nm), which is expected to result in good compatibility with presently available imaging instrumentation using standard optical equipment (laser, filter, dichroic mirror) for Cy5.

For selective Ca^{2+} recognition and binding, the most well-known Ca^{2+} chelating moiety, BAPTA (*O*,*O*′-bis(2-aminophenyl)ethyleneglycol-*N*,*N*,*N*′,*N*′-tetra acetic acid), was selected owing to its excellent selectivity for Ca^{2+} over other ions.[12] Grafting BAPTA on KFL-5 is expected to invoke a photoinduced electron transfer (PET) from the electron-rich ion chelating moiety to the fluorescent dye moiety.[13] In the absence of Ca^{2+}, the fluorescence of KFL is likely quenched due to this PET process, and emission is expected to recover upon binding to Ca^{2+}, because of the weakening of the electron-donating ability of the BAPTA moiety. To enhance the water solubility, two additional carboxyl moieties were introduced into the KFL core *via* methylene chains.

[a] *Department of Applied Chemistry, Faculty of Science and Technology, Keio University, 3-14-1, Hiyoshi, Kohoku-ku, Yokohama 223-8522, Japan. E-mail: suzuki@applc.keio.ac.jp; Fax: +81 45-566-1566*
[b] *Department of Biosciences and Informatics, Faculty of Science and Technology, Keio University, 3-14-1, Hiyoshi, Kohoku-ku, Yokohama 223-8522, Japan. E-mail: oka@bio.keio.ac.jp*
† Electronic supplementary information (ESI) available: Further experimental details and data. See DOI: 10.1039/c1cc14045k

As shown in Fig. 1b, the absorption band of KFCA is located in the far-red to NIR region (λ_{max} = 655 nm) and not essentially influenced by the presence or absence of Ca^{2+} (0 or 39 μM Ca^{2+}). Bright NIR emission (λ_{max}: 670 nm, ϕ = 0.24) was observed with a sharp fluorescence spectral band (full width at half-maximum height: $\Delta\lambda_{1/2}$ = 33 nm) in the presence of Ca^{2+} (39 μM), while basically no fluorescence was measurable (ϕ < 0.002) in the absence of Ca^{2+}. The ON/OFF fluorescence signal contrast (120-fold) is extraordinarily high compared to those of cyanine-based (<4-fold) and squaraine-based Ca^{2+} probes (~3 fold). It reaches almost the same level as Fluo-4, which is one of the most widely used Ca^{2+} probes (Table 1).

As expected from the optical properties of the KFL-5 fluorophore, the absorption/fluorescence emission wavelengths are almost identical to the commercially available Cy5. The fluorescence emission intensity Ca^{2+}-titration plot of KFCA in buffered aqueous solution well fitted the theoretical sigmoidal response curve calculated based on a 1 : 1 complex formation (Fig. 1c). The calculated K_d value (500 nM, Fig. S1 in the ESI†) is almost the same as that of a typical methyl-modified BAPTA compound like Fluo-4,[12] indicating that the binding affinity and characteristics of BAPTA are retained on conjugation to the KFL fluorophore. Finally, KFCA has a high molar extinction coefficient (ε = 180 000 M^{-1} cm^{-1}). Although BODIPY-based probes are sometimes less soluble in water owing to their hydrophobic BODIPY core, KFCA has relatively high water solubility (>1 mM without the use of any cosolvent).

Encouraged by these particular optical properties, especially the brightness and the excellent ON/OFF ratio, the usefulness of KFCA for biological application was investigated, focusing on intracellular Ca^{2+} imaging. KFCA (1 μM) was introduced into HeLa cells by the beads-loading method.[14,15] After a short period of incubation (15 min), KFCA was well accumulated in the cytoplasm, and its fluorescence signal could be detected by using a typical excitation laser and filter set for Cy5 (see the ESI†).

In order to reveal the applicability of KFCA for dual imaging in combination with typical visible-light-emitting fluorescent probes, the signal crosstalk between KFCA and other fluorescent probes or proteins (Fluo-4 and DsRed2) was evaluated. First, HeLa cells were stained by either Fluo-4 or KFCA, respectively, and their fluorescence was observed. As shown in Fig. 2a, fluorescence of Fluo-4 (ex. 488 nm) was observed only in the fluorescein channel (500–545 nm), while no signal was captured in the Cy5 channel (655–755 nm). On the other hand, fluorescence of KFCA (ex. 635 nm) was only captured in the Cy5 channel, showing the possibility of complete signal separation.

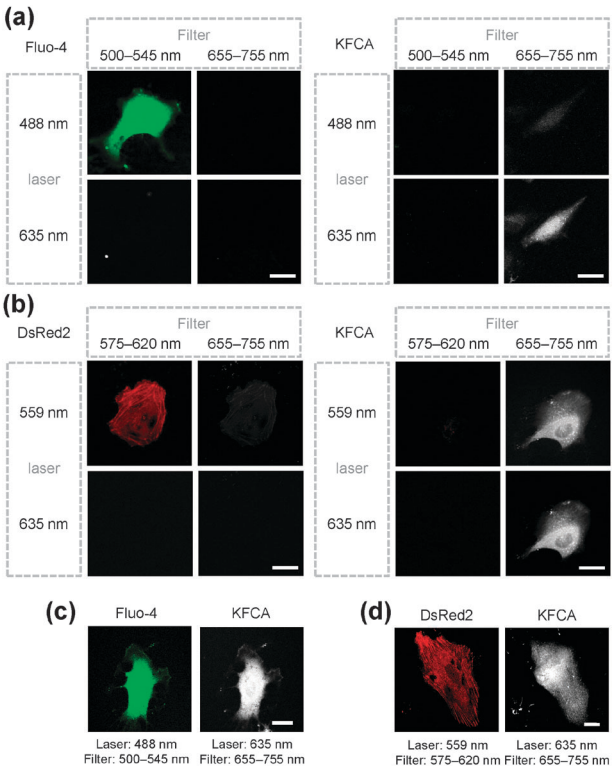

Fig. 2 Signal crosstalk of KFCA and other fluorophores: (a) fluorescence images of HeLa cells loaded with Fluo-4 or KFCA; scale bar, 10 μm. (b) Fluorescence images of HeLa cells expressing DsRed2-actin or loaded with KFCA; scale bar, 20 μm. (c) Fluorescence images of HeLa cells loaded with both Fluo-4 and KFCA; scale bar, 20 μm. (d) Fluorescence images of HeLa cells expressing DsRed2-actin and loaded with KFCA; scale bar, 20 μm.

Similar, and remarkable results were also obtained in terms of the red fluorescent protein DsRed2 (ex./em. = 558/583 nm) in Fig. 2b. Fluorescence of the DsRed2 protein (ex. 559 nm) expressed on the actin filament in the HeLa cells was observed in the DsRed2 channel (575–620 nm), whereas no fluorescence signal was captured in the Cy5 channel (655–755 nm). On the other hand, KFCA in HeLa cells without DsRed2 protein could be excited by 635 nm lasers, and its fluorescence was detected only in the Cy5 channel. DsRed2 is widely used not only as a fluorescent marker for specific organelles or proteins, but also as a suitable resonance energy transfer (RET)-acceptor in combination with many green or yellow fluorescent proteins due to its long-wavelength emission property. Hence, the fact that KFCA shows no crosstalk with DsRed2 indicates that it can be used in combination with most fluorescent proteins for various imaging purposes. Furthermore, these results prove the usefulness of KFCA as an orthogonal

Table 1 K_d values and optical properties of KFCA and some reported fluorescent probes

	K_d/μM	ϕ_{free}	ϕ_{bound}	ON/OFF contrast (F_{bound}/F_{free})	Reference
KFCA	0.50	0.002[a]	0.24	120	—
Cyanine	0.24	0.05	0.12	<4	8
Squaraine	3.6	n.d.[b]	n.d.	3	9
Fluo-4	0.35	n.d.	0.14	120	14

[a] Estimated from the following calculation: $\phi_{free} = \phi_{bound} \times (F_{free}/F_{bound})$, F denotes the fluorescence integral. [b] No data.

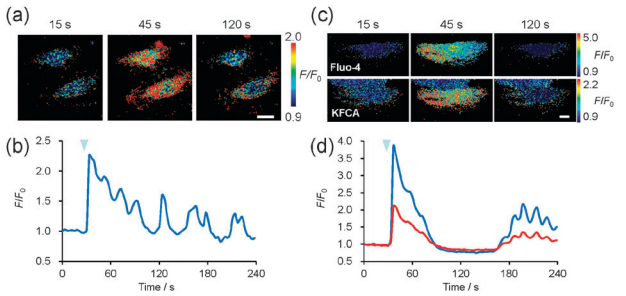

Fig. 3 Real-time single- or dual-colour Ca^{2+} imaging: (a) pseudo-coloured images of KFCA-loaded HeLa cells with ATP stimulation (100 μM) at 30 s. Images were captured at 15 s, 45 s, and 120 s; scale bar, 20 μm. (b) Time course of fluorescence change of KFCA. The arrowhead indicates the timing of ATP addition. (c) Pseudocoloured images of HeLa cells loaded with both Fluo-4 and KFCA with ATP stimulation (100 μM) at 30 s. Upper and lower figures represent the imaging data of Fluo-4 (laser: 488 nm, filter: 500–545 nm) and KFCA (laser: 635 nm, filter: 655–755 nm), respectively. Images were captured at 15 s, 45 s, and 120 s, respectively; scale bar, 20 μm. (d) Time course of fluorescence change of Fluo-4 (blue) and KFCA (red). The arrowhead indicates the timing of ATP addition.

fluorescent probe to most of the presently available visible-light-emissive probes including orange or red fluorophores. On the basis of these results, co-staining of HeLa cells with Fluo-4 and KFCA (Fig. 2c), and also staining of DsRed2-actin-expressed HeLa cells with KFCA (Fig. 2d) were performed. The fluorescent signals of each fluorophore could be distinguished in the different channels using different sets of excitation lasers and emission filters without any signal crosstalk.

Next, the usefulness of KFCA for monitoring intracellular calcium concentrations $[Ca^{2+}]_i$ was evaluated. As shown in Fig. 3a and b and in Video S1 in the ESI†, the addition of 100 μM ATP (a reagent leading to an increase in $[Ca^{2+}]_i$) caused a significant increase in the fluorescence emission (F/F_0, up to 250%) with time-related changes (including oscillation).[16] Stimulation by 5 μM ionomycin (a reagent causing a cytosolic Ca^{2+} increase) also resulted in increasing fluorescence emission (Fig. S2 and Video S2 in the ESI†). These fluorescence emission intensity changes observed with KFCA well agreed with the data obtained by using Fluo-4 (Fig. S3 and S4 and Videos S3 and S4 in the ESI†), emphasising that the emission intensity changes of KFCA correspond to the changes of the Ca^{2+} concentrations. According to the literature, the ON/OFF ratio (dynamic range) of typical Ca^{2+} indicators (*e.g.* Fluo-4, Calcium Green, Calcium Orange, Oregon Green 488 BAPTA-1) in cells tends to be a few times (sometimes over one digit) lower than those *in vitro*.[17] For this reason, the observed F/F_0 value is considered to be consistent.

Finally, dual staining of HeLa cells by both KFCA and Fluo-4 and dual-colour real-time $[Ca^{2+}]_i$ monitoring were performed. After stimulation by ATP (100 μM), completely identical fluorescence emission patterns with oscillation (corresponding to Ca^{2+} oscillation) were observed from KFCA and Fluo-4 (Fig. 3c and d and Video S5 in the ESI†). These results reveal not only that the fluorescent signal of KFCA clearly reflects the intracellular calcium behaviour, but also that KFCA is fully compatible for real-time multiplexed imaging in combination with typical visible-light-emitting probes.

For these reasons, the present results make KFCA a promising new tool for various advanced Ca^{2+} imaging applications (*e.g.* simultaneous real-time bioimaging of multiple targets using numerous fluorescent sensors and fluorescent protein sensors, *in vivo* calcium imaging), which are difficult or impossible to be performed using existing fluorescent Ca^{2+} probes. Additionally, KFCA as the first example of a fluorescent probe derived from the KFL fluorophores reveals their potential in the development of fluorescent sensors. Therefore, the design of NIR fluorescent probes for other target ions or for reactive oxygen species (ROS) is possible based on this study.

This work was supported by a JSPS stipend to K.U. and a Grant-in-Aid for Scientific Research (A) from the Ministry of Education, Culture, Sports, Science and Technology, Japan (No. 20245019). We acknowledge T. Nagai (Hokkaido Univ.) and M. Kamiya (Univ. Tokyo) for supporting us with the beads-loading method, and Y. Hiruta (Keio Univ.) for his help with NMR data acquisition.

Notes and references

1 R. Y. Tsien, *Biochemistry*, 1980, **19**, 2396–2404.
2 A. Miyawaki, J. Llopis, R. Heim, J. M. McCaffery, J. A. Adams, M. Ikura and R. Y. Tsien, *Nature*, 1997, **388**, 882–887.
3 H. M. Kim, B. R. Kim, M. J. An, J. H. Hong, K. J. Lee and B. R. Cho, *Chem.–Eur. J.*, 2008, **14**, 2075–2083.
4 H. W. Ai, K. L. Hazelwood, M. W. Davidson and R. E. Campbell, *Nat. Methods*, 2008, **5**, 401–403.
5 W. Tomosugi, T. Matsuda, T. Tani, T. Nemoto, I. Kotera, K. Saito, K. Horikawa and T. Nagai, *Nat. Methods*, 2009, **6**, 351–353.
6 Y. Niino, K. Hotta and K. Oka, *PLoS One*, 2009, **4**, e6036.
7 R. Weissleder, *Nat. Biotechnol.*, 2001, **19**, 316–317.
8 B. Ozmen and E. U. Akkaya, *Tetrahedron Lett.*, 2000, **41**, 9185–9188.
9 E. U. Akkaya and S. Turkyilmaz, *Tetrahedron Lett.*, 1997, **38**, 4513–4516.
10 K. Umezawa, Y. Nakamura, H. Makino, D. Citterio and K. Suzuki, *J. Am. Chem. Soc.*, 2008, **130**, 1550–1551.
11 K. Umezawa, A. Matsui, Y. Nakamura, D. Citterio and K. Suzuki, *Chem.–Eur. J.*, 2009, **15**, 1096–1106.
12 A. Takahashi, P. Camacho, J. D. Lechleiter and B. Herman, *Physiol. Rev.*, 1999, **79**, 1089–1125.
13 A. P. deSilva, H. Q. N. Gunaratne, T. Gunnlaugsson, A. J. M. Huxley, C. P. McCoy, J. T. Rademacher and T. E. Rice, *Chem. Rev.*, 1997, **97**, 1515–1566.
14 M. Kamiya and K. Johnsson, *Anal. Chem.*, 2010, **82**, 6472–6479.
15 P. L. McNeil and E. Warder, *J. Cell Sci.*, 1987, **88**, 669–678.
16 M. J. Berridge, M. D. Bootman and P. Lipp, *Nature*, 1998, **395**, 645–648.
17 D. Thomas, S. C. Tovey, T. J. Collins, M. D. Bootman, M. J. Berridge and P. Lipp, *Cell Calcium*, 2000, **28**, 213–223.